Properties of Hydrogels Derived from Cationic Analogues of Bile Acid: Remarkably Distinct Flowing Characteristics

Neralagatta M. Sangeetha,[†] Shreedhar Bhat,[†] Angshuman R. Choudhury,[†] Uday Maitra,[†] and Pierre Terech*[,‡]

Department of Organic Chemistry, Indian Institute of Science, Bangalore 560 012, India, and UMR5819 CEA-CNRS-University J. Fourier, DRFMC-SI3M-PCM, CEA-Grenoble 17, rue des Martyrs, 38054 Grenoble Cedex 9, France

Received: June 23, 2004

A new class of cationic bile acid derivatives was synthesized to gel water and aqueous electrolyte solutions. Investigations on these hydrogels are carried out at different length scales by a combination of physical techniques. Each of these hydrogels exhibits unique characteristics, thus providing a spectrum of thermal, optical, and mechanical properties. X-ray crystallographic investigation of the single crystals of two of the gelators shows significant differences in the solid-state packing. X-ray scattering experiments indicate that the gel state consists of a different morph than that in the solid. Electron microscopic investigations of the xerogels reveal the fibrous nature of the gel structure. These fibers are associated mainly through bundling processes. A detailed rheological study reveals significant differences in the mechanical properties of the three hydrogels. The storage modulus varies in the range $(0.2-2) \times 10^5$ Pa at $C = 2$ wt % for these systems. The exponents of the scaling of the rheological parameters with the concentration for two of the systems agree well with those expected for cellular solids or strongly interacting colloidal gels. A third system exhibits a singular behavior with the energy of interaction between the colloidal flocs increasing with the concentration.

1. Introduction

Low molecular mass gels have been receiving considerable attention in recent years. This interest stems not only from their implied potential in various technological applications[1,2] but also from the fundamental viewpoint of understanding their supramolecular structures at different length scales and the properties thereof. In the class of low-mass gels, the reported examples of hydrogelators[3−21,22] are fewer in comparison to that of organogelators. While the organogelators aggregate in organic media via a variety of associative mechanisms, such as H-bonding, $\pi-\pi$ interaction, charge-transfer interaction, London dispersion forces, and involve a great diversity of molecular structures, hydrogelators are amphiphilic molecules, generally derived from natural products, and their association in aqueous media is mainly driven by hydrophobic interactions. The majority of studies in this field concerns delineation of the essential structural features that renders a particular chemical entity a gelator and/or the determination of the molecular architecture within the gel fibers. There are very few reports that discuss the flowing properties of such systems.[18,23−25] These rheological studies are essential to understand the fundamental relations among the structures of the fibers, their junction zones at different length scales, and the mechanical cohesion of their networks. They are also important to evaluate the suitability of the gel systems for potential applications. This report presents a comparative study of the properties of gels derived from three cationic derivatives, NMM-DC, NMP-DC, and DABCO-DC, corresponding to the *N*-methylmorpholine, *N*-methylpyrrolidine, and DABCO salts derived from 24-nor-23-iodo-3,12-dihydroxycholane, respectively (Chart 1). The distinct macroscopic properties (thermal, optical, and mainly flowing properties) exhibited by the gels derived from these three derivatives, which differ from each other only in the nature of the headgroup, is remarkable. In the class, the NMM-DC gels present a singular behavior that is also emphasized by comparison with the rheological properties of other known molecular gels. The collection of rheological data is analyzed in the light of theoretical models that relate the macroscopic properties to the structure of the gels.

CHART 1: Cationic Bile Acid Derivatives

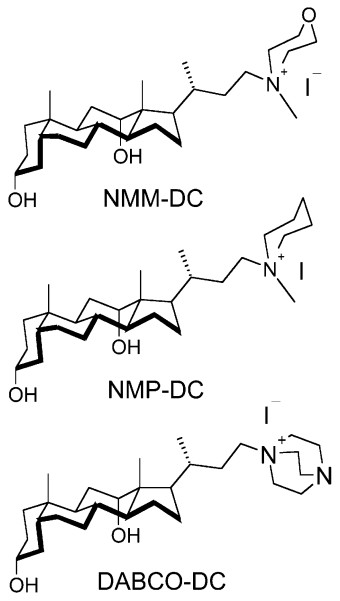

* Corresponding author. Tel: +33 4 38 78 59 98. Fax: +33 4 38 78 56 91. E-mail: pterech@cea.fr.
[†] Indian Institute of Science.
[‡] UMR5819 CEA-CNRS-University J. Fourier.

10.1021/jp047272z CCC: $27.50
Published on Web 09/04/2004

SCHEME 1: Synthesis of the Gelators (see the text)[a]

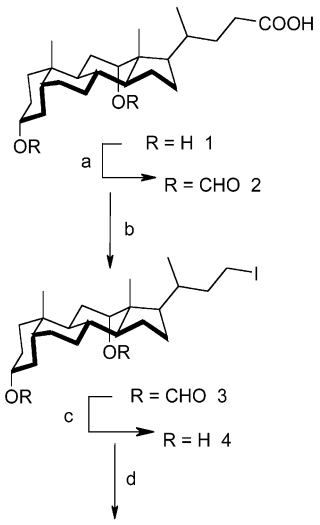

[a] Reaction conditions: (a) HCOOH, 55 °C, 90%; (b) I_2, $Pb(OAc)_4$, 63%; (c) K_2CO_3, MeOH, THF, 90%; (d) NMM, NMP, or DABCO, CH_3CN, 70−80%.

2. Results and Discussions

2.1. Synthesis. The synthesis of gelators is carried out as outlined in Scheme 1.[26] Deoxycholic acid **1** is converted to its diformyl derivative **2** (90%) by heating with formic acid at 50 °C.[27] A Hunsdiecker type reaction of **2** with $Pb(OAc)_4$ and iodine in CCl_4 gives the 24-nor-23-iodo derivative **3** (65%),[28] which is deformylated (K_2CO_3/MeOH) to obtain **4** (95%). Reaction of **4** with *N*-methylmorpholine, *N*-methylpiperidine, and 1,4-diazabicyclo[2,2,2]octane (DABCO) in refluxing MeCN yielded salts NMM-DC, NMP-DC, and DABCO-DC, respectively. The crude salts are crystallized from MeOH or EtOH/$CHCl_3$ to yield 75−80% of the pure salts.

2.2. Aggregation Properties. The critical micellar concentrations (cmc) of these salts are determined using pyrene as the fluorescent probe.[29,30] The cmc values measured in 0.5 M NaCl at 25 ± 1 °C for the surfactants NMM-DC, NMP-DC, and DABCO-DC are comparable and equal to 2.8, 2.3, and 2.5 mM, respectively. It should be noted that the primary stages of the aggregation described by the cmc do not distinguish the systems.

Surfactants NMM-DC, NMP-DC, and DABCO-DC form stable, thermoreversible gels in aqueous salt solutions (0−4 M NaCl). They can also gel 1 M solutions of salts such as Na_2CO_3, NaBr, Na_2SO_4, and KCl. Gels formed at lower concentration of the gelator and NaCl are transparent and turn progressively translucent when the concentration of either of these is increased. For the present study, a constant concentration $C_{NaCl} = 0.5$ M is arbitrarily chosen. The ability to form gels in 0.5 M NaCl solution is illustrated with the partial phase diagram shown in Figure 1. First points are closest to the critical gelation concentration (below this limit, the material remains soluble). In the concentrated range, the last points are not the upper limits for the systems. The thermal stability of the gels increases with the concentration of the gelator, as expected. The gel to sol transition temperature (T_{gs}) for the gels follows the order NMP-DC > NMM-DC > DABCO-DC.[31] There is no trivial relation between the melting temperature of the gels (T_{gs}) and the high melting temperature of the pure solids (on the order of 265−290 °C; see the Experimental Section) obtained under nongelling conditions. The enthalpy of disaggregation is calculated from

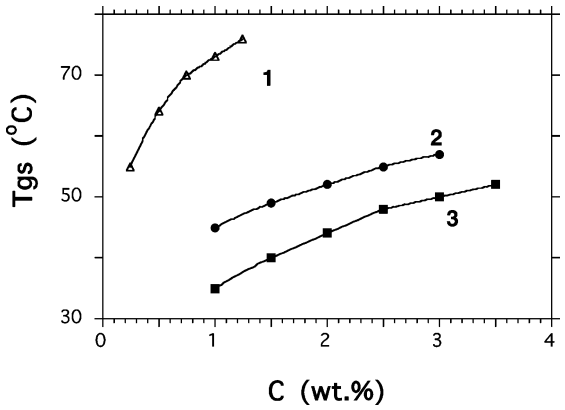

Figure 1. Gel to sol phase diagram for gels of NMP-DC (1), NMM-DC (2), and DABCO-DC (3) in 0.5 M NaCl.

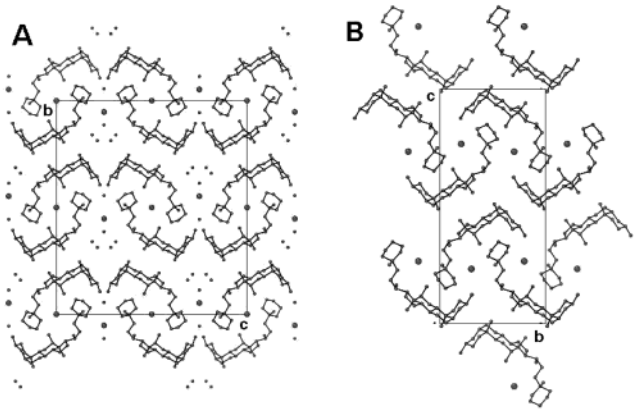

Figure 2. Crystallographic organization in NMP-DC (A) and NMM-DC (B) crystals.

plots of ln(C) versus $1/T_{SG}$ using the Schröeder van Laar equation $\ln(C) = -\Delta H/RT_{GS} + C$. ΔH values are 79, 72, and 60 kJ mol^{-1} for gels of NMM-DC, NMP-DC, and DABCO-DC, respectively.

There are significant differences in the optical appearance of the gels derived from these gelators. The gels of NMP-DC and DABCO-DC are more translucent as compared to those of NMM-DC. Also, the gels of NMP-DC are more rigid and resistant to mechanical shaking than are the other two. A striking difference in the macroscopic cohesion of the gels is also observed between the three gels. When subjected to mechanical agitation, gels of NMM-DC (typically at $C \sim 1-2\%$ w/v) break into a slurry of small aggregates (globular), while the gels derived from the other two break into larger lumps. Thus, gels of NMM-DC exhibit a lower cohesion at a macroscopic level. At this stage, the unique macroscopic aspects and behaviors that characterize each of the systems are already noticeable. The relative turbidity and fragility of NMM-DC gels seems to be a singular situation that may be clarified from data obtained by other techniques (vide infra).

The crystallographic organization of the gelator molecules within the pure solids (obtained from nongelling conditions) can be considered for NMM-DC and NMP-DC (see Figure 2A,B). Both systems exhibit bilayered structures with hydrophobic interactions between their lipophilic faces. NMM-DC crystallizes in an orthorhombic $P2_12_12_1$ crystallographic space group with $a = 7.3187$ Å, $b = 13.1932$ Å, $c = 29.3297$ Å ($Z = 4$, density d is 1.35) with no water molecules entrapped in the unit cell. NMP-DC crystallizes in a different orthorhombic crystallographic habitus, $C222_1$ with $a = 7.0402$ Å, $b = 31.9476$

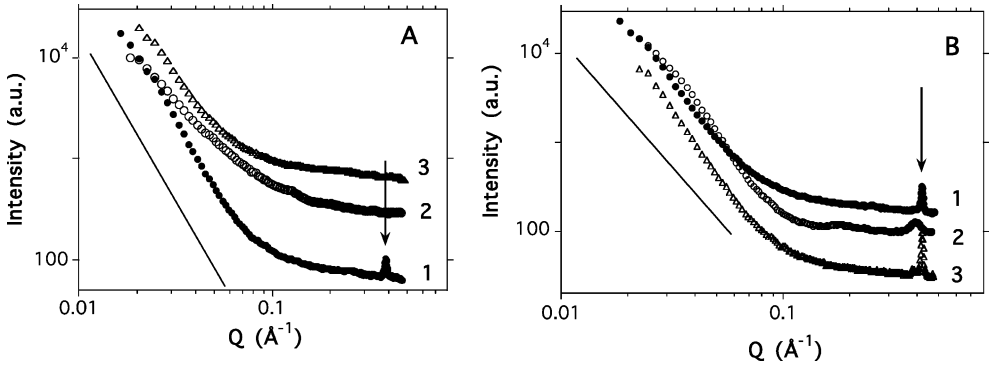

Figure 3. SAXS profiles for the crystalline powder (1), the swollen gel (2), and the dried gel (3) for NMP-DC (A) and NMM-DC (B). The arrow points at a major Bragg peak observed with the crystalline powder of the gelator.

Å, $c = 28.3755$ Å ($Z = 8$, $d \sim 1.39$) and four water molecules included per gelator. NMP-DC adopts a zigzagged bilayer organization with molecules in each layer arranged in a head-to-head and tail-to-tail fashion. The formed strands run antiparallel to the adjacent layer and give complementary head-to-tail arranged molecular pairs. In the hydrophobic layer, the C-3 hydroxyl of one molecule is H-bonded with the C-3 hydroxyl of the adjacent one ($d_{H\cdots O} = 2.008$ Å and O−H···O angle = 165.7°). Cavities embedding a cluster of water molecules are scattered over the lipophilic layer. Conversely, NMM-DC exhibits zigzagged bilayers with head-to-tail arrangements of molecules in each layer, devoid of cavities and H-bonds. These differences in molecular organizations do not affect significantly the internal cohesive energy and the related melting points (see Experimental Section). However, the thermal stability of NMP-DC gels stands remarkably higher than that of NMM-DC. These observations suggest a significant modification of the crystalline morph in the gels.

Support for such a hypothesis can be obtained from a preliminary small-angle X-ray scattering (SAXS) experiment. SAXS profiles in Figures 3A,B show that the intense Bragg peak typical of the crystalline state, at $Q = 0.38$ Å^{-1} (NMP-DC) or 0.43 Å^{-1} (NMM-DC), is absent in the NMP-DC gel and broadened and shifted to a low-Q value in NMM-DC gels (while found identically in the xerogel). Broad bumps or an enlarged peak seen in the range 0.1−0.25 Å^{-1} for both NMP-DC and NMM-DC gels also suggests a change of morph in the gel state. Redistribution of the H-bonds in a gelator on moving from the solid state to a swollen gel has already been observed in different systems.[32,33] Also, for organogel systems involving no H-bonding, the differences in molecular packing between the gel, xerogel and neat solid phases have been clearly demonstrated.[34−36] For example, the packing of a modified-androstanol steroid derivative evolves from an orthorhombic $P2_12_12_1$ organization in the solid to a monoclinic one in the organogel.[35] Differences in molecular packing between a wet organogel and a xerogel have also been characterized in some imidazole derivatives.[36] Differences in the packing modes are leading to minor variations in the enthalpy of disaggregation ΔH (see Figure 1) but can also affect the Young's modulus of fibers to which some mechanical properties are sensitive. Rheological properties depend also on the spatial distribution of fibers in the network, as shown in the following.

2.3. Optical Microscopy. The optical textures exhibited by the three gels in 1 mm quartz cells under a polarizing optical microscope are shown in Figure 4A−C. The observed textures suggest that gels prepared under these conditions are composed of a patchwork of anisotropic domains with defects. The optical pattern of each of the gels was unlike each other, which is indicative of differences in the microscopic organization of the gel networks. The size of the domains is in the sequence DABCO-DC < NMM-DC < NMP-DC. The texture observed with NMP-DC is reminiscent of Schlieren textures observed for systems composed of threadlike organizations.

2.4. Scanning Electron Microscopy. The scanning electron micrographs in Figure 5 show the existence of fibrillar species in the gels. Solid specimens (xerogels) for SEM experiments were obtained by solvent evaporation of a gel deposit on a silicon wafer. Under these kinetic conditions, various mechanisms, such as nucleation-growth reactions, epitaxial growths, bundle formations, and collapse/shrinkages of the networks, take part in the formation of a porous mesh. The micrographs (Figures 5) show heterogeneous, random networks of connected fibers. Interestingly, no supramolecular chirality is discernible in the fiber architecture, although they are formed from chiral steroids. The balance between self-avoiding trajectories of the fibers and bundling processes that results in the final supramolecular architecture needs to be further analyzed with a probing technique operating at larger length scales. Rheometry appears appropriate to estimate the level of interactions between these fibrillar colloidal aggregates.

2.5. Rheology. Cationic DC systems are studied by dynamic rheology. Gels are viscoelastic and hence both store and dissipate mechanical energy. In oscillatory experiments, the viscoelasticity is characterized by the dynamic storage modulus G' and the loss modulus G'', being defined as the ratios of stress in-phase and out-of-phase, respectively, to an imposed oscillatory deformation. Frequency sweep experiments performed at a fixed stress in the linear domain of deformations are analyzed first. Figure 6 presents the variation of the dynamic moduli and complex viscosity as a function of the oscillatory frequency for a gel of NMM-DC. The dynamic elastic modulus G' stands larger than the loss modulus at all frequencies, as expected for soft solids. Similar curves are obtained for the other two gels. While the ratio G'/G'' is more than 10 for NMM-DC and NMP-DC gels, it is around 4−6 for DABCO-DC gels, indicating that dissipation of energy through viscous mechanisms is more predominant with DABCO-DC gels. Consistently, the frequency sweep exhibits a significantly sloped G' vs f (see Table 1), suggesting slow rearrangements in the gels. The complex viscosity does not show any Newtonian plateau at low frequencies and decays with a slope of −1. Such mechanical behavior is characteristic of soft viscoelastic solids, and the three cationic DC systems can be qualified as gels.[37]

The flowing response of NMM-DC and NMP-DC gels to an ascending stress ramp is presented in Figure 7A,B. These curves are useful for the estimation of the linear viscoelastic domain, where Hooke's law holds and the elastic modulus is independent

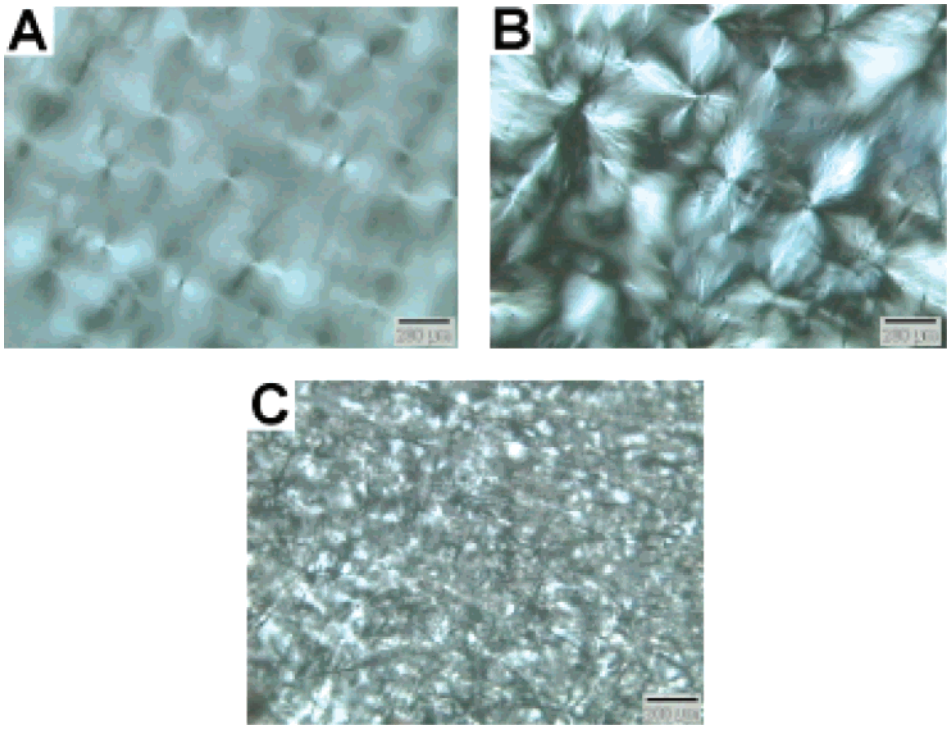

Figure 4. Optical micrographs of gels of DABCO-DC (A), NMM-DC (B), NMP-DC (C) prepared in 0.5 M NaCl aqueous solutions (1 mm quartz cells).

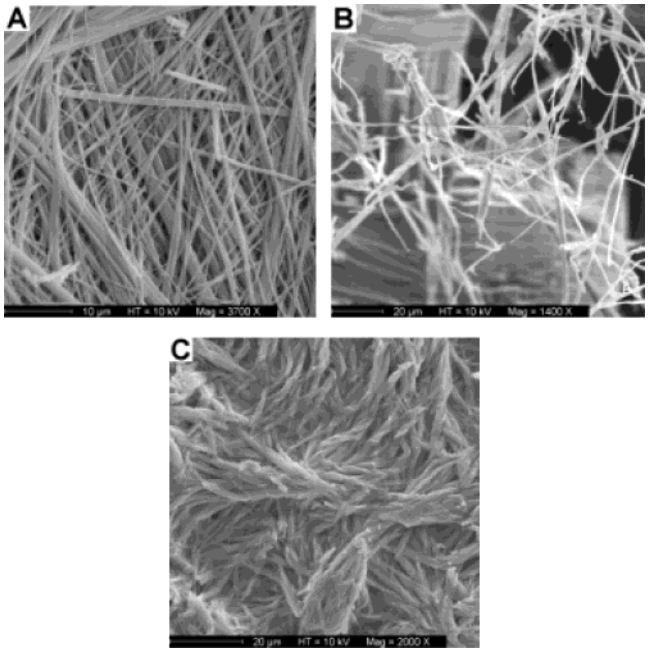

Figure 5. SEM of cationic DC-xerogels: NMM-DC (A) obtained from a gel in 0.5 M NaCl; NMP-DC (B) obtained from a gel in 0.5 M NaCl; DABCO-DC (C) obtained from a gel in 0.15 M NaCl. The scale bar is indicated.

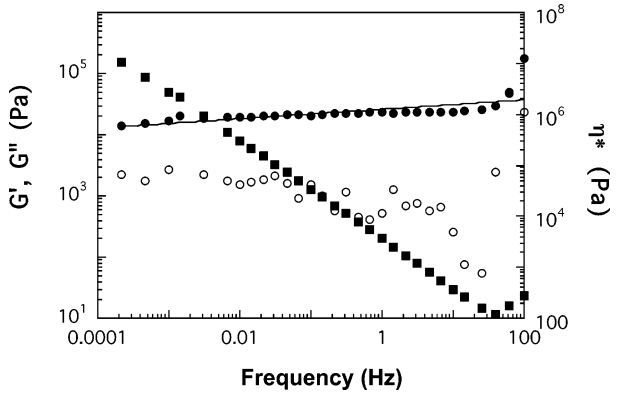

Figure 6. Typical frequency sweep experiment for a NMM-DC hydrogel (C = 2% w/v, 0.5 NaCl).

of the applied stress. The linear regime is limited to small strain of ≤1% for NMM-DC gels in 0.5 M NaCl. Gels of DABCO-DC show similar profiles (not shown), with the limit of linearity, γ_0, being restricted to a lower strain of ≤0.7%. A strikingly different behavior is observed with NMP-DC gels. At concentrations $C \geq 1.6\%$ w/v, gels present linear viscoelastic regimes ($\gamma_0 \sim 1\%$), and for $C \leq 1.2\%$ w/v, there is no linearity in the measured moduli. The partially deformed gels, however, exhibit a plateau over a strain range, which extends on either side of 1% strain, which is notable. A closer examination of the variation of the limit of linearity γ_0 with the concentration of NMM-DC gels is useful (in experiments carefully performed to maintain a constant stress rate). It reveals a small, progressive increase in the linear domain with concentration (Figure 7A), followed by a soft decrease. This variation of γ_0 with the concentration can be related to the theoretical behavior expected for some colloidal gels (vide infra).[38,39]

Typical curves for the dependence of G' with the applied oscillatory stress ($f = 1$ Hz) from which σ^* values are extracted are shown in Figure 8. Above σ^*, the gel fails and flow occurs. A comparison of the G' and σ^* values for gels of the three gelators gives the sequence NMP-DC > DABCO-DC ≥ NMM-DC. Lower values of G' and σ^* for NMM-DC gels is consistent with previous visual observations of the relative fragility of the gel upon shaking. Interestingly, the elasticity of gels of NMM-DC is lower than that of DABCO-DC in the concentration range 1.5−3% w/v and is comparable to that of NMM-DC at higher concentrations.

The strength and elasticity of the cationic DC gels are higher as compared to those of sodium deoxycholate aqueous gels

TABLE 1: Typical Rheological Data for the DC-Hydrogels[a]

compound	concn, % w/v	G' (Pa)	G'' (Pa)	δ^* (Pa)	G'/G''	m of $G' = kf^m$	n of $G' = kC^n$	p of $\delta^* = kC^p$
NMP-DC	2.0	3.07×10^5	13580	2660	22.6	0.025	1.97	1.83
NMM-DC	2.0	23200	1240	375	18.6	0.041	3.47	3.15
DABCO-DC	2.0	69000	16000	780	4.3	0.073	2.13	2.03

[a] The scaling laws and their related exponents are presented for G' versus the frequency of the applied stress (m), G' versus concentration (n), and yield stress versus concentration (p).

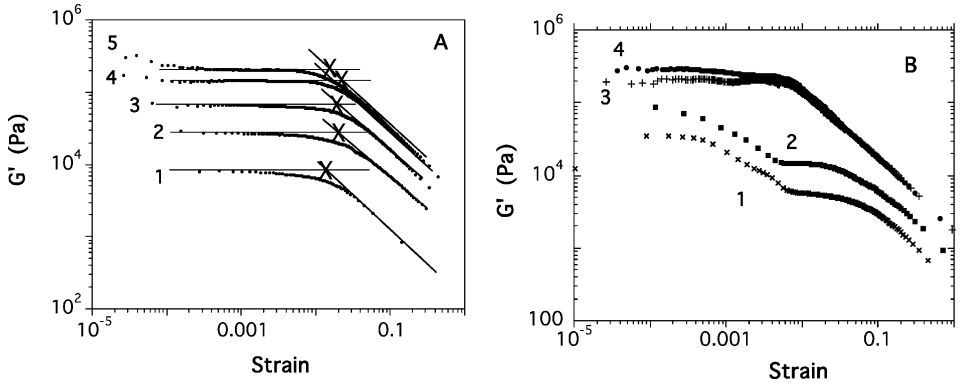

Figure 7. Variation of the elastic shear modulus of cationic DC-hydrogels as a function of the applied strain ($f = 1$ Hz). (A): NMM-DC in 0.5 M NaCl: (1) 1.5% w/v; (2) 2.0% w/v; (3) 3.0% w/v; (4) 4.0% w/v; (5) 5% w/v. Crosses (x) indicate the corresponding yield stress values (σ^*). (B) NMP-DC in 0.5 M NaCl: (1) 0.75% w/v; (2) 1.2% w/v; (3) 1.6% w/v; (4) 2.0% w/v.

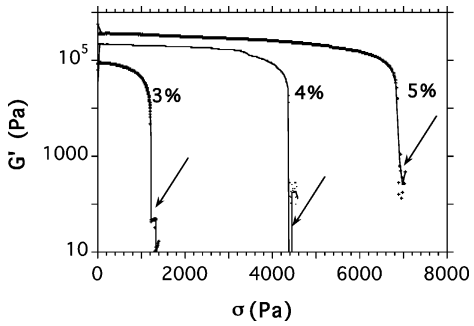

Figure 8. Typical stress sweep experiments for NMM-DC hydrogels at three concentrations. The value of the yield stress σ^* is estimated (see arrows) from the sharp decrease of the elastic shear modulus G' (frequency $f = 1$ Hz).

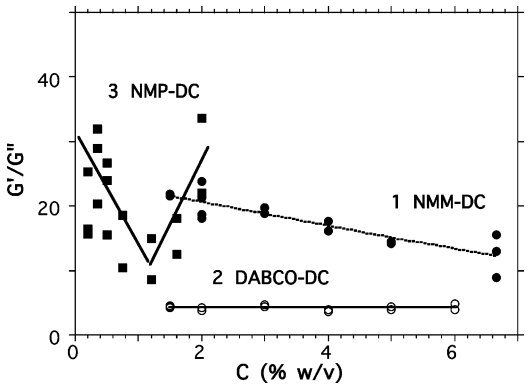

Figure 9. Variations of the G'/G'' ratio as a function of the hydrogelator concentration (see text) for the three systems.

(from which the DC systems are primarily derived). The latter exhibit a very pH-dependent strength, and to illustrate, $G' =$ 60 Pa ($f = 3.18$ Hz) at $C \sim 4.8\%$ w/v and pH = 6.8 (concentration of sodium phosphate of 0.0232 mol dm^{-3}).[25] For comparison, NMM-DC hydrogels are more than 3 orders of magnitude stiffer than the deoxycholate gels! Indeed, at $C =$ 3.0% w/v, NMM-DC gel has a storage modulus G' (1 Hz) of 88 300 Pa and fails at $\sigma^* \sim 1200$ Pa. The rheological properties of cationic DC-hydrogels can also be compared to those of low-molecular mass organogels (at $C \sim 1.0\%$ w/v). For example, a bis-urea-based organogel in 1-hexanol exhibits an equilibrium $G' \sim 40\,000$ Pa,[24] and a nitrobenzene gel of 12-hydroxystearic acid has a shear elasticity of ca. 40 190 Pa,[23] while NMP-DC gel has $G' \sim 73\,000$ Pa.

The profile for the variation of G'/G'' as a function of the gelator concentration (Figure 9), which can be considered as an estimation of the stiffness of the gels, also discriminates the three cationic DC gels. DABCO-DC gels exhibit a flat profile at relatively low value of stiffness. NMM-DC gels have a larger rigidity that progressively decreases with concentration. NMP-DC gels that exhibit the largest elasticity present also a minimum in its stiffness. This phenomenology points at the existence of a variable balance of fiber association mechanisms (bundle formations, average mesh size, mean diameters, etc.) from one system to the other. Eventually, the scaling laws of the elastic shear modulus and yield stress of the three gelators as a function of the concentration (or $C -$ cmc), G' vs C^n and σ^* vs C^p, can be estimated as shown in Figure 10A. These scaling exponents exemplify the way the elasticity of a representative unit (i.e., floc or cell) in a gel is transduced through the macroscopic structure. Values of the corresponding exponents are collected in Tables 1 and 2. For the shear elasticity of NMP-DC and DABCO-DC gels, the exponent n is around 2, while with NMM-DC hydrogels, n is significantly larger (3.5). A refined analysis of the scaling profile for the NMM-DC gels divulges two slopes (Figure 10B). At low concentrations, the slope corresponds to $n \sim 5$, while at higher concentrations it corresponds to $n \sim$ 2.8. This behavior singles out the NMM-DC gels from the class. Elasticity (G'), fragility (σ^*), and stiffness (G'/G'') of gels are inter-related parameters ($\sigma^* = \gamma_c G'$, γ_c being the critical deformation) and result from the interplay between specific static and dynamic mechanisms for fiber interaction.

The rheological data can be mainly considered within three theoretical contexts.

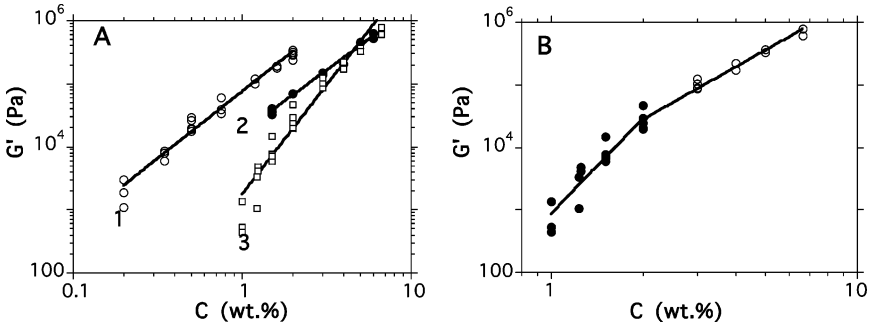

Figure 10. (A) Scaling laws of the elastic shear modulus G' as a function of the concentration for NMP-DC (1), DABCO (2), and NMM-DC (3) hydrogels. Full lines are best fits for $G' = kC^n$. Values of the corresponding exponents n are collected in Table 1. (B) Refined analysis for NMM-DC hydrogels. Full circles correspond to a regime with an exponent $n = 5.05$ and open circles are for a concentrated regime with $n = 2.76$.

First, the cationic DC systems can be considered as colloidal gels involving floclike elements. The packing of fractal flocs leads to typical behaviors of the domain of linearity γ_0 and elasticity G' versus the concentration,[39,38] depending upon the relative strength of the inter- and intrafloc links. Mainly, two regimes can be defined: weak- and strong-link regimes. In the strong-link regime, the elasticity of a floc is dominated by its effective backbone, i.e., a linear chain of springs. The interfloc links are stronger than the intrafloc links and the elasticity of the intrafloc links gives the resulting elasticity of the gel. The exponent n is then deduced from expression 1

$$n = (d + x)/(d - d_f) \quad (1)$$

where d is the Euclidean dimension of the system, d_f is the fractal dimension of the floc, and x is the fractal dimension of the backbones forming the flocs. In the weak-link regime, the elasticity of the gel is determined by the elasticity of the interfloc links that are less rigid than the flocs themselves and the exponent n is deduced from expression 2

$$n = 1/(d - d_f) \quad (2)$$

Experimentally, if the strong-link regime is considered, the elasticity of a floc is dominated by its effective backbone, i.e., a linear chain of springs. Then eq 1 prevails. Assuming $x = 1$ (as expected for fibers), $n = 2$ when the fractal dimension of the floc is $d_f = 1$. This value of the exponent is well observed with NMP- and DABCO-DC gels (see Tables 1 and 2).

With NMM-DC gels in the concentration range 1−2%, the exponent for the storage modulus scaling relation is $n \sim 5$. The combination of the observation of an exponent different from 2 of the G' vs C scaling law and that of fibers by SEM (accounting for the description of the linear backbones of the flocs) is a good argument to consider the colloidal gel model involving fractal flocs as a possible theoretical context. It appears that $n \sim 5$ is similar to the exponent observed for whey protein in salted gels ($n \sim 5$)[40] and comparable to that obtained for boehmite alumina gels ($n \sim 4.2$).[38] The trend of a decreasing limit of linearity with increasing concentration indicated that the latter alumina gel system was in the strong-link regime. With NMM-DC gels, the variation of γ_0 with increasing concentration shows a soft increase followed by a soft decrease and thus supports the trend of an evolution of the system from the class of weak-link regime toward that of a strong-link regime.[39] A corresponding evolution of the fractal dimension from 2.8 (Table 2, column 4) to 1.55 (Table 2, column 3) is then deduced. Notably, the "weak-link regime" seems to be consistent with the visual observation of the fragility of NMM-DC gels upon shaking.

TABLE 2: Comparisons with Theoretical Models for Colloidal Gels[48]

			d_f [b]	
compound	n[a]	p[a]	strong ($x = 1$[c])	weak
NMP-DC	1.99	1.82	0.62	2.50
NMM-DC[d]	5.05 & 2.76 or 3.46	5.16 & 2.80 or 3.52	2.21 & 1.55 or 1.84	2.80 & 2.64 or 2.71
DABCO-DC	2.04	2.03	1.04	2.51

[a] n and p are the exponents for the scaling of the storage modulus and yield stress, respectively, with concentration. [b] d_f is the resulting fractal dimension using expressions 1 or 2 respectively for strong or weak interaction between the flocs. [c] $x = 1$ is the fractal dimension of the skeleton of fibrillar flocs. [d] For NMM-DC, the analysis is made considering either the average value of n or each of the two concentration regimes (see the text).

A second possible theoretical context for the analysis of the rheological properties considers the network formation as resulting more from a crystallization process than from an aggregation phenomenon. The ramified growth of networks is considered to be resulting from homogeneous branching with a constant branching rate of ca. 2.[41] A specialized fractal context ("trimmed Cayley tree") is then used to describe the branching as the determinant step in the network growth. The branching by self-epitaxial nucleation of daughter branches on a growing parent branch is referred to as a "noncrystallographic branching" process. Using this context, a fractal dimension ($d_f \sim 2.4$) for the self-similar pattern of the spatial distribution of fibers has been obtained for a low-mass organogel from rheological and light scattering measurements.[42] With cationic DC-hydrogels, there is no clear evidence from SEM data that such a branching process can be prevalent. The SEM picture displayed by Figures 5 is more of a mesh of interpenetrated fibers and bundles. Such bundles may be formed either after the fiber growth or simultaneously via a double nucleation mechanism.[43]

A third theoretical context available to describe the mechanical properties of such gel networks is that of cellular solids[44] formed with beams, struts, and hinges exhibiting plastic deformations out of the linear viscoelastic regime. If the network is made up of stiff elements joined at fixed cross-link points (energetic network rather than entropic), the theory[45] predicts that the elastic modulus, mainly fixed by the Young's modulus of the gelator and the section and length between two nodes, should vary as C^2. Clearly, DABCO- and NMP-DC gels, having an exponent $n \sim 2$, can be described in such a context. An identical behavior is also observed with various organogels as for instance with either a 12-hydroxystearic acid[23] system or a bis-urea-based organogel.[24] It is interesting to note that the model gives a similar prediction of a colloidal gel context with flocs having a linear backbone in a strong-link interaction regime.

3. Conclusion

The three cationic DC aqueous systems are robust gels characterized by high elasticities and yield stress values. Interestingly, each of the systems exhibits a unique behavior in terms of its thermal, optical, and mechanical properties. Elastic moduli of gels obtained from these cationic derivatives are 2−3 orders of magnitude larger than those observed for sodium deoxycholate at comparable concentrations. The elastic moduli are however comparable to the ones reported for organogels derived from low-mass compounds.[23,24,46] The SEM analysis of dried gels shows fibers of finite radii and indeterminate lengths either bundled (Figure 5A) or intertwined (Figure 5C), revealing no branching. Mechanical entanglements seem to be the dominant force preventing the macroscopic flow over large time scales. Most of DC-hydrogels behave as cellular solids: this is the situation for NMP- and DABCO-DC hydrogels. NMM-DC shows a very particular behavior since the $G' = kC^2$ scaling law (k being a proportionality constant) is not observed. We have shown that the theoretical context of colloidal gels with interacting flocs could also be used to account for the "ordinary" quadratic scaling law that corresponds to a strong interaction regime with fibrillar flocs. The variation of the values of the exponent n and that of the linearity domain with the NMM-DC concentration supports the description of the system as undergoing a modification of the interaction level between flocs from the weak to the strong link regimes. The modification is accompanied with a variation of the fractal dimension from 2.8 to 1.55. More compact structures would develop at low concentrations. Such a behavior has also been observed with gels obtained with spherical particles derived from a fluorinated polymer[47] and also with gels formed by salt-induced aggregation of polystyrene spheres.[48] Nevertheless, the theoretical validation of such a tendency remains controversial.[48,49] Interestingly, more turbid gels are observed in NMM-DC compare to NMP- or DABCO-DC systems. It remains that the present work presents a first attempt to analyze the rheology of molecular hydrogels within the different theoretical contexts available. Low (or ultralow)-angle scattering experiments are planned to investigate the structure factor of the systems so as to confirm the self-similarity structural relationship and the associated fractal dimension of the representative structural unit in the gel (floc).

4. Experimental Section

Physical Measurements. Rheological measurements were made on a Haake RS100 stress-rheometer. A plate−plate geometry (diameter 20 mm) with striations was used in order to avoid slippage between the plates and the gel.[23] The gap between plates was 0.6 mm for all measurements. The sample was introduced between the plate in the form of a hot sol. After confirmation of the completion of gelation, followed by measuring the dynamic moduli as a function of time (2−3 h) at a very small applied stress, the experiments were performed. Covering the measuring cell with a glass cap limited evaporation of the solvent during measurements. The temperature of the sample was maintained with an accuracy of 0.1 °C. The determination of the linear viscoelastic regime of deformations and yield stress of the gels were done by dynamic measurements at a frequency of 1 Hz of the oscillatory stress. Optical micrographs of the gels in 1 mm quartz cells were recorded between crossed polarizers at a magnification of 10×, on an Olympus BX100 optical microscope. SEM experiments were done on a JEOL JSM 840A microscope at an accelerating voltage of 10 keV. The xerogels were sputtered with a 200 Å thick gold layer before observation. The gel to sol transition temperatures (T_{gs}) of the gels were measured by the inverted tube method. Gels prepared in sealed test tubes (0.8 cm diameter, 0.5 mL of gel) were kept upside down in a thermostat, and the temperature was varied slowly (0.2 °C/min). The temperature at which the gel falls under gravity was noted as the T_{gs}. Uncertainty in the measured T_{gs} was ±1 °C. Fluorescence measurements were done on a Perkin-Elmer LS-50B luminescence spectrometer in 2 or 5 mm square quartz tubes. X-ray scattering profiles were obtained on a rotating anode (wavelength = 1.5418 Å) using a Kα/Kβ filtered beam and focused by two curved Franks mirrors.

Synthetic Procedures. *3α,12-Bis(formyloxy)-7-deoxy-5β-cholanic Acid (**2**).* A suspension of 7-deoxycholic acid **1** (12 g, 30 mmol) in formic acid (98−100%) (40 mL, 10.6 mol) was stirred for 4 h at 55 °C and the solvent removed in a vacuum. The residue was recrystallized from 80% EtOH/H_2O to yield 12.3 g (89%) of the product. ^{1}H NMR ($CDCl_3$, 300 MHz) δ: 0.73 (s, 3 H), 0.82 (d, J = 6.0 Hz, 3 H), 0.90 (s, 3 H), 1.92−2.43 (m, steroidal CH, CH_2), 4.81 (m, 1 H), 5.23 (s, 1 H), 8.01 (s, 1 H), 8.11 (s, 1 H).

*24-Nor-23-iodo-3α,12α-bis(formyloxy)-7-deoxy-5β-cholane (**3**).* A suspension of **2** (5.5 g, 11 mmol) and $Pb(OAc)_4$ (12 g, 27 mmol) in CCl_4 (20 mL) was heated to reflux under argon. A solution of iodine (5 g, 19.6 mmol) in CCl_4 (90 mL) was added dropwise while the solution was irradiated with two 100 W tungsten lamps. The addition was continued (∼ 2 h) till the color of iodine persisted. The reaction mixture was refluxed for an additional 30 min and filtered through Celite. The filtrate was washed with a 5% sodium thiosulfate solution and dried over anhydrous Na_2SO_4. The crude mixture obtained on evaporation of the solvent was chromatographed on a silica gel column using 5−15% EtOAc/hexane to yield 4.6 g (68%) of the product. ^{1}H NMR ($CDCl_3$, 300 MHz) δ: 0.77 (s, 3 H), 0.84 (d, J = 6.3 Hz, 3 H), 0.93 (s, 3 H), 1.00−2.05 (m, steroidal CH, CH_2), 3.05 (m, 1 H), 3.30 (m, 1 H), 4.83 (m, 1 H), 5.25 (s, 1 H), 8.03 (s, 1 H), 8.13 (s, 1 H).

*24-Nor-23-iodo-3α,12α-dihydroxy-7-deoxy-5β-cholane (**4**).* To a solution of compound **3** (2.2 g, 3.9 mmol) in MeOH−THF (3:2, 25 mL) was added K_2CO_3 (4 g, 29 mmol) and the mixture stirred at room temperature. After 15 h, the reaction mixture was filtered and solvent removed in vacuo. Water (50 mL) was added to the residue, and the mixture was extracted with ethyl acetate, washed with water, dilute chlorhydric acid, and brine, and dried over anhydrous Na_2SO_4. The crude product obtained on evaporation of the solvent was purified on a silica gel column (19 cm × 3.2 cm) using 30−50% EtOAc/hexane to yield 1.7 g (91%) of the product. ^{1}H NMR ($CDCl_3$, 300 MHz) δ: 0.69 (s, 3 H), 0.91 (s, 3 H), 0.97 (d, J = 6.0 Hz, 3 H), 1.02−2.17 (m, steroidal CH, CH_2), 2.04 (m, 1 H), 3.11 (m, 1 H), 3.34 (m, 1 H), 3.61 (m, 1 H), 3.98 (s, 1 H).

N-Methylmorpholinium Salt of 24-Nor-23-iodo-3α,12α-dihydroxy-7-deoxy-5β-cholane (NMM-DC). A suspension of **4** (1 g, 2.11 mmol) in CH_3CN (10 mL) was heated to reflux, *N*-methylmorpholine (2 mL, 18.12 mmol) was added, and refluxing was continued for 6 h. Solvent was removed in vacuo and the crude product was purified on a silica gel column using 25−85% EtOH/$CHCl_3$. The pure product weighed 850 mg (70%). Mp: 268−269 °C. $[\alpha]^{25}_D$: 39.4 (*c* 1.32, EtOH). IR (KBr, cm^{-1}): 3414, 2959, 2924, 2861, 1634, 1471, 1458, 1380, 1300, 1251. ^{1}H NMR (300 MHz, DMSO-d_6) δ: 0.60 (s, 3H), 0.83 (s, 3H), 0.98 (d, J = 5.7 Hz, 3H), 1.03−1.80 (m, steroidal CH, CH_2), 3.12 (s, 3H), 3.78 (br s, 1H), 3.91 (br s, 4H), 4.24 (d, J = 2.7 Hz, 1H), 4.50 (d, J = 2.7 Hz, 1H). ^{13}C NMR (75 MHz, DMSO-d_6) δ: 12.37, 17.41, 23.08, 23.43, 26.11, 26.64, 26.98, 27.06, 28.58, 30.21, 32.95, 33.53, 33.81, 35.14, 35.67, 36.24,

41.59, 45.41, 45.92, 46.08, 47.53, 58.71, 59.17, 59.86, 62.91, 69.87, 70.97. FAB-MS: calcd 448.3790, obsd 448.3775. Anal. Calcd for $C_{28}H_{50}NO_3I$: C, 58.43; H, 8.76; N, 2.43. Found: C, 58.08; H, 8.83; N, 2.05.

N-Methylpiperidinium Salt of 24-Nor-23-iodo-3α,12α-dihydroxy-7-deoxy-5β-cholane (NMP-DC). To a suspension of **4** (0.5 g, 1.05 mmol) in CH_3CN (5 mL) heated to reflux was added *N*-methylpiperidine (1 mL, 8.3 mmol), and refluxing was continued for 9 h. Solvent was evaporated and the crude product obtained was purified on a silica column using 25−85% EtOH/$CHCl_3$. The pure compound weighed 300 mg (50%). Mp: 264−266 °C. $[\alpha]^{25}_D$: 35.9 (*c* 1.98, EtOH). IR (KBr, cm^{-1}): 3445, 2945, 2866, 1625, 1470, 1446, 1370, 1302, 1230, 1042. ^{1}H NMR (300 MHz, DMSO-d_6) δ: 0.61 (s, 3H), 0.84 (s, 3H), 0.99 (d, J = 6.9 Hz, 3H), 1.03−1.82 (m, steroidal CH, CH_2), 3.00 (s, 3H), 3.34 (br s, 6H), 3.79 (s, 1H), 4.26 (unresolved doublet, 1H), 4.49 (unresolved doublet, 1H). ^{13}C NMR (75 MHz, DMSO-d_6) δ: 12.34, 17.42, 19.32, 20.71, 23.08, 23.41, 26.09, 26.84, 26.95, 27.05, 28.55, 30.21, 32.90, 33.53, 33.79, 35.12, 35.62, 36.24, 41.55, 45.83, 46.03, 46.46, 47.50, 59.63, 60.03, 69.90, 70.89. FAB-MS: calcd 446.3998, obsd. 446.3978. Anal. Calcd for $C_{29}H_{52}NO_2I\cdot H_2O$: C, 58.90; H, 9.20; N, 2.37. Found: C, 58.93; H, 9.22; N, 1.97.

Diazabicyclo[2.2.2]octanium Salt of 24-Nor-23-iodo-3α,12α-dihydroxy-7-deoxy-5β-cholane (DABCO-DC). To a refluxing suspension of **4** (1 g, 2.11 mmol) in CH_3CN (10 mL) was added diazabicyclo[2.2.2]octane (0.3 g, 2.54 mmol), and reflux continued for an additional 4 h. The solvent was evaporated and the crude product was dissolved in 10 mL of ethanol by heating. To this ethanolic solution was added diethyl ether dropwise until a white solid precipitated out. The solid was recrystallized from acetonitrile. The pure compound weighed 1.04 g (83%). Mp: 296−297 °C. $[\alpha]^{25}_D$: 39.0 (*c* 1.0, EtOH). IR (KBr, cm^{-1}): 3454, 2920, 2860, 1462, 1383, 1091, 1055, 1043, 843. ^{1}H NMR (300 MHz, DMSO-d_6) δ: 0.60 (s, 3H), 0.84 (s, 3H), 0.96 (d, J = 5 Hz, 3H), 1.01−1.81 (steroidal CH, CH_2), 3.00 (br s, 6H), 3.29 (br s, 6H), 3.77 (s, 1H), 4.34 (d, J = 3.6 Hz, 1H), 4.55 (d, J = 3.6 Hz, 1H). ^{13}C NMR (75 MHz, DMSO-d_6) δ: 12.35, 17.33, 23.08, 23.40, 26.09, 26.87, 26.95, 27.03, 28.544 30.19, 32.91, 33.55, 33.80, 35.12, 35.62, 36.25, 41.56, 44.73, 45.74, 46.03, 47.50, 51.32, 61.44, 69.87, 70.85, 79.30. LRMS: 459.46 (M^+). Anal. Calcd for $C_{29}H_{51}N_2O_2I$: C, 59.38; H, 8.76; N, 4.78. Found: C, 59.58; H, 8.80; N, 4.91.

Acknowledgment. The present work has been possible thanks to the support of the Indo-French Center for Promotion of Advanced Research (IFCPAR project 2605-1), which is deeply thanked. Dr. A. de Geyer and J. J. Allegraud are acknowledged for their valuable help in the SAXS and SEM experiments, respectively.

Note Added after ASAP Posting. This paper was published ASAP on September 4, 2004, without Angshuman R. Choudhury listed as an author. The corrected version was posted September 20, 2004.

References and Notes

(1) Terech, P.; Weiss, R. G. *Chem. Rev.* **1997**, *97*, 3133−3159.
(2) Abdallah, D. J.; Weiss, R. G. *Adv. Mater.* **2000**, *12*, 1237−1247.
(3) Gortner, R. A.; Hoffman, W. F. *J. Am. Chem. Soc.* **1921**, *43*, 2199.
(4) Brenzinger, Z. *Physiol. Chem.* **1892**, *16*, 537.
(5) Amis, E. S.; La Mer, V. K. *Science* **1939**, *90*, 90−91.
(6) Pfannemuller, B.; Welte, W. *Chem. Phys. Lipids* **1985**, *37*, 227−240.
(7) Fuhrhop, J.-H.; Schneider, P.; Rosenberg, J.; Boekema, E. *J. Am. Chem. Soc.* **1987**, *109*, 3387−3390.
(8) Newkome, G. R.; Baker, G. R.; Arai, S.; Saunders, M. J.; Russo, P. S.; Theriot, K. J.; Moorefield, C. N.; Rogers, L. E.; Miller, J. E.; Lieux, T. R.; Murray, M. E.; Phillips, B.; Pascal, L. *J. Am. Chem. Soc.* **1990**, *112*, 8458−8465.
(9) Hamada, H.; Yamada, K.; Mitsuishi, M.; Ohira, M.; Miyazaki, K. *J. Chem. Soc., Chem. Commun.* **1992**, 544.
(10) Bhattacharya, S.; Acharya, S. N. G. *Chem. Mater.* **1999**, *11*, 3121−3132.
(11) Franceschi, S.; de Viguerie, N.; Riviere, M.; Lattes, A. *New. J. Chem.* **1999**, *23*, 447−452.
(12) Makarevic, J.; Jokic, M.; Peric, B.; Tomisic, V.; Kojic-Prodic, B.; Zinic, M. *Chem. Eur. J.* **2001**, *7*, 3328.
(13) Oda, R.; Huc, I.; Candau, S. J. *Angew. Chem., Int. Ed.* **1998**, *37*, 2689.
(14) Iwaura, R.; Yoshida, K.; Masuda, M.; Yase, K.; Shimizu, T. *Chem. Mater.* **2002**, *14*, 3047−3053.
(15) Haines, S. R.; Harrison, R. G. *Chem. Commun.* **2002**, 2846−2847.
(16) Marmillon, C.; Gauffe, F.; Bulik-Krzywicki, T.; Loup, C.; Caminade, A.-M.; Majoral, J.-P.; Vors, J.-P.; Rump, E. *Angew. Chem., Int. Ed.* **2001**, *40*, 2626−2629.
(17) Maitra, U.; Mukhopadhyay, S.; Sarkar, A.; Rao, P.; Indi, S. S. *Angew. Chem., Int. Ed.* **2001**, *40*, 2281.
(18) Menger, F. M.; Caran, K. L. *J. Am. Chem. Soc.* **2000**, *122*, 11679−11691.
(19) Suzuki, M.; Yumoto, M.; Kimura, M.; Shirai, H.; Hanabusa, K. *Chem. Commun.* **2002**, 884−885.
(20) Estroff, L. A.; Hamilton, A. D. *Angew. Chem., Int. Ed.* **2000**, *39*, 3447−3450.
(21) Kobayashi, H.; Friggeri, A.; Koumoto, K.; Amaike, M.; Shinkai, S.; Reinhoudt, D. N. *Org. Lett.* **2002**, *4*, 1423−1426.
(22) Estroff, L. A.; Hamilton, A. D. *Chem. Rev.* **2004**, *104*, 1201−1217.
(23) Terech, P.; Pasquier, D.; Bordas, V.; Rossat, C. *Langmuir* **2000**, *16*, 4485−4494.
(24) Brinksma, J.; Feringa, B. L.; Kellogg, R. M.; Vreeker, R.; van Esch, J. *Langmuir* **2000**, *16*, 9249−9255.
(25) Jover, A.; Meijide, F.; Nunez, E. R.; Tato, J. V. *Langmuir* **2002**, *18*, 987−991.
(26) Sangeetha, N. M.; Balasubramanian, R.; Maitra, U.; Ghosh, S.; Raju, A. R. *Langmuir* **2002**, *18*, 7154−7157.
(27) Cortese, F.; Bauman, L. *J. Biol. Chem.* **1936**, *113*, 779−785.
(28) Ahmed, S.; Alauddin, M.; Caddy, B.; Martin-Smith, M.; Sidwell, W. T. L.; Watson, T. R. *Aust. J. Chem.* **1971**, *24*, 521.
(29) Kalyanasundaram, K.; Thomas, J. K. *J. Am. Chem. Soc.* **1977**, *99*, 2039−2044.
(30) Gouin, S.; Zhu, X. X. *Langmuir* **1998**, *14*, 4025.
(31) Measured by inverted tube method: Murata, K.; Aoki, M.; Nishi, T.; A., I.; Shinkai, S. J. C. S. *Chem. Commun.* **1991**, 1715. *J. Chem. Soc., Chem. Commun.* **1991**, 1715.
(32) Menger, F. M.; Yamasaki, Y.; Catlin, K. K.; Nishimi, T. *Angew. Chem., Int. Ed. Engl.* **1995**, *34*, 585−586.
(33) van Esch, J.; Schoonbeek, F.; de Loos, M.; Kooijman, H.; Spek., A. L.; Kellog, R. M.; Feringa, B. L. *Chem. Eur. J.* **1999**, *5*, 937−950.
(34) Ostuni, E.; Kamaras, P.; Weiss, R. G. *Angew. Chem., Int. Ed. Engl.* **1996**, *35*, 1324−1326.
(35) Terech, P.; Rodriguez, V. *Prog. Colloid Polym. Sci.* **1994**, *97*, 151−153.
(36) Ballabh, A.; Trivedi, D. R.; Dastidar, P. *Chem. Mater.* **2003**, *15*, 2136−2140.
(37) Terech, P. Gels. In *Encyclopedia of Surface Colloid Science*; Dekker, I., Ed.; Dekker: New York, 2002.
(38) Shih, W.-H.; Shih, W. Y.; Kim, S.-I.; Liu, J.; Aksay, I. A. *Phys. Rev. A* **1990**, *42*, 4772−4779.
(39) Wu, H.; Morbidelli, M. *Langmuir* **2001**, *17*, 1030−1036.
(40) Verheul, M.; Roefs, S. P. F. M.; Mellema, J.; de Kruif, K. G. *Langmuir* **1998**, *14*, 2263−2268.
(41) Liu, X. Y.; Sawant, P. D. *App. Phys. Lett.* **2001**, *79*, 3518−3520.
(42) Liu, X. Y.; Sawant, P. D. *Adv. Mater.* **2002**, *14*, 421−426.
(43) Ferrone, F. A.; Hofrichter, J.; Eaton, W. A. *J. Mol. Biol.* **1985**, *183*, 611−631.
(44) Leon, E. J.; Verma, N.; Zhang, S.; Lauffenburger, D. A.; Kamm, R. D. *J. Biomater. Sci. Polymer Ed.* **1998**, *9*, 297−312.
(45) Jones, J. L.; Marques, C. M. *J. Phys. Fr.* **1990**, *51*, 1113−1127.
(46) Schmidt, R.; Schmutz, M.; Mathias, A.; Decher, G.; Michel, R.; Mésini, P. J. *Langmuir* **2002**, *18*, 7167−7173.
(47) Lattuada, M.; Wu, H.; Morbidelli, M. *Phys. Rev. E* **2001**, *64*, 061404−1−7.
(48) Carpinetti, M.; Ferri, F.; Giglio, M.; Paganini, E.; Perini, U. *Phys. Rev. A* **1990**, *42*, 7347−7354.
(49) Gonzalez, A. E.; Lach-Hab, M.; Blaisten-Barojas, E. *J. Sol-Gel Sci. Technol.* **1999**, *15*, 119−127.